

## Pyrolysis Characteristic of Tobacco Stem Studied by Py-GC/MS, TG-FTIR, and TG-MS

Bei Liu,<sup>a, b</sup> You-Ming Li,<sup>a, b\*</sup> Shu-Bin Wu,<sup>b</sup> Yan-Heng Li,<sup>c</sup> Shan-Shan Deng,<sup>c</sup> and Zheng-Lin Xia<sup>d</sup>

Pyrolysis characteristics and mechanism of tobacco stem were studied by pyrolysis coupled with gas chromatography/mass spectrometry (Py-GC/MS), thermogravimetric analyzer coupled with Fourier transform infrared spectrometry, and mass spectrometry (TG-FTIR and TG-MS) techniques. The composition of evolved volatiles from fast pyrolysis of tobacco stem was determined by Py-GC/MS analysis, and the evolution patterns of the major products were investigated by TG-FTIR and TG-MS. Py-GC/MS data indicated that furfural and phenol were the major products in low temperature pyrolysis, and these were generated from depolymerization of cellulose. Indene and naphthalene were the major products in high temperature pyrolysis. TG-FTIR and TG-MS results showed that CO, CO<sub>2</sub>, phenols, aldehydes, and ketones were released between 167°C and 500°C; at temperatures >500°C, CO and CO<sub>2</sub> were the main gaseous products.

*Keywords:* Tobacco stem; Pyrolysis; TG-FTIR; TG-MS; PY-GC/MS

*Contact information:* a: National Engineering Research of Papermaking and Pollution Control, South China University of Technology, Guangzhou 510640, China; b: State Key Laboratory of Pulp and Paper Engineering, South China University of Technology, Guangzhou 510640, China; c: Guangdong Province Tobacco Quality Supervision and Test Station, Guangzhou 510635, China; d: Guangdong Jinye Tobacco Slice Technology Development Co. Ltd., Shantou 515600, China; \*Corresponding author: ymli3@scut.edu.cn

### INTRODUCTION

Nowadays biomass-containing wastes, such as agricultural and industrial wastes, have begun to supplement energy and materials needs in place of fossil fuels (Li *et al.* 2008; Purwono *et al.* 2011; Xia *et al.* 2011; Yang *et al.* 2012). Tobacco stem is a typical by-product of the tobacco manufacturing process (Piotrowska *et al.* 2009; Kayikçioğlu and Okur 2011). The major components of tobacco stem are cellulose, lignin, and hemicellulose, each of which can be effectively utilized for other purposes. The amount of tobacco stem generated in China was greater than 1.5 million tons in 2008 (Xia *et al.* 2011). However, most of the tobacco stem waste is either discarded or incinerated, which can adversely affect the environment as well as human health. So, it is meaningful to explore new technologies to better utilize tobacco stem.

Recently, many researchers have explored novel approaches for utilizing tobacco stem waste. There have been some studies on the pyrolysis of tobacco stem in order to produce activated carbons. Up to now, the strong effects of different factors, such as activation agents, heating rates, and activation methods, on the use of tobacco stem for activated carbon production have been investigated. In addition, a number of studies have illustrated the thermochemical conversion processes of tobacco stem as an alternative means of converting this waste into more valuable fuel products. For instance, Ahamad

and Alshehri (2012) investigated the evolved products of bidi tobacco powder by using TG-FTIR-MS technique. The author concluded that the main gases and volatile products released during the combustion and pyrolysis are CO, CO<sub>2</sub>, NH<sub>3</sub>, HCN, NO, isoprene, formaldehyde, acetaldehyde, acrolein, *etc.* Sung and Seo (2009) studied the thermal behavior of tobacco stem on a thermogravimetric analyzer (TGA) both in air and in N<sub>2</sub>, and the authors reported that decomposition conditions and tobacco species had significant effect on the mass loss patterns. Li *et al.* (2011) studied the co-combustion thermal behavior of high-ash anthracite coal, tobacco residue, and their blends on TGA under different temperatures. The author concluded that the combustion of tobacco residue was controlled by the emission of volatile matter, and tobacco residue obviously improved the combustion characteristics of high-ash anthracite coal. Meanwhile, the authors proposed a method that could enable the co-combustion of tobacco residue and high-ash anthracite coal as an alternative fuel source. Pütün *et al.* (2007) studied the product yields and compositions of tobacco residue for both slow and fast pyrolysis in a fixed bed; the authors suggested that the obtained bio-oils from pyrolysis could be used as conventional fuels.

Based on the review of these previous studies, it was discovered that the properties of volatiles products components and emission patterns of tobacco stem pyrolysis have not been clearly investigated. It is well known that the products characteristics of biomass pyrolysis play a decisive role in the viability of a biomass being used for bio-chemicals and bio-fuels (Mohan *et al.* 2006; Czernik and Bridgwater 2004; French and Czernik 2010; Heo *et al.* 2010). Therefore, further research work is required to improve the understanding of tobacco stem pyrolysis products properties and evolution patterns. The objective of this study was to investigate the evolution patterns of volatiles and the pyrolysis products characteristics of tobacco stem by thermogravimetric/Fourier transform infrared spectroscopy (TG-FTIR), thermogravimetric/mass spectroscopy (TG-MS), and pyrolysis-gas chromatography/mass spectrometry (Py-GC/MS).

## EXPERIMENTAL

### Materials

Tobacco stems used in this study were collected from Guizhou Province, P.R. China. The fresh raw samples were washed thoroughly with deionized water, and then dried at 60°C, crushed and sieved with a 120-mesh screen.

**Table 1.** Characteristics of the Feedstock

Proximate Analysis (%)	Volatiles	Fixed Carbon	Ashes	Moisture
	67.85	17.55	5.20	9.40
Ultimate Analysis (%)	C	H	S	N
	46.01	8.54	0.34	0.81
Chemical Analysis (%)	Cellulose	Hemicellulose	Lignin	
	39.01	5.05	6.51	

The proximate analysis was carried out according to ASTM D 3172 -1989 (International Association for Testing Materials). The CHNS elemental analysis of the samples was performed with an elements analyzer (Vario-I Germany). The component analysis was done according to the TAPPI standard methods (Technical Association of the Pulp and Paper Industry, USA). The results are shown in Table 1.

## Methods

### *TG-FTIR method*

A Jupiter Thermogravimetric Analyzer STA 449 F3 coupled with a Thermo Electron Corporation Fourier transformation infrared spectrometer TENSOR 27 was used. The experiments were done on the TGA at a heating rate of 20°C/min. within the temperature range from 50 to 1000°C, and high purity nitrogen was used as carrier gas with a flow rate of 20 mL/min. Volatile products evolved from TGA were led into the FTIR gas cell through a heated stainless steel transfer line kept at  $T = 150^{\circ}\text{C}$ . The spectrum was obtained in the range 4000 to 667  $\text{cm}^{-1}$  and the resolution factor was set at 4  $\text{cm}^{-1}$ .

### *Py-GC/MS method*

Fast pyrolysis of tobacco stem was carried out in a Chemical Data System (CDS5150, USA) analytical flash pyrolyzer. The pyrolyzer consisted of an inductively heated coil to heat the samples at the heating rate of 10 °C/ms from room temperature to different temperatures of 400°C, 500°C, 600°C, 700°C, and 800°C. Pyrolysis reactions were carried out with an event time of 0.5 s, and the obtained pyrolysis products were analyzed by a gas chromatograph (QP2010, Japan) and an electron impact mass spectroscopy (EI-MS) analyzer. Data processing were performed with the Perkin Elmer NIST spec version 05.

### *TG-MS method*

The TG experiments were performed in a Jupiter Thermogravimetric Analyzer at a heating rate of 20°C/min up to a final temperature of 1000°C under the high purity nitrogen flow rate of 20 mL/min. Mass spectra of the gases evolved from TGA were recorded by a QS422 (Pfeiffer Vacuum Instrument) quadruple mass spectrometer. The transfer lines between the TGA and MS were heated to 200°C in order to avoid cold spots and thus prevent the condensation of the gaseous products. The mass spectrometer was operated at 70 eV. The m/z was carried out from 1 to 100 amu to determine which m/z has to be specified during the TG experiments. The ion curves that were close to the noise level were omitted. Finally, only the intensities of 15 selected ions (m/z = 94, 96, 106, 108, 116, 124, and 128) were monitored with the thermogravimetric parameters.

## RESULTS AND DISCUSSION

### **Py-GC/MS Analysis of the Components of Evolved Volatiles**

Fast pyrolysis temperature of tobacco stem was set at 400°C, 500°C, 600°C, 700°C, and 800°C, and obtained pyrolysis products were detected with GC/MS. The identification and relative molar abundances of the released products are shown in Table 2. Relative peak areas were calculated for pyrolysis products, and the summed areas of

the peaks were normalized to 100%. From the data in Table 2 the main products from tobacco stem pyrolysis at 400°C were identified as: furfural, guaiacol, phenol, and 2-cyclopenten-1-one. Furfural was the dominating pyrolysate in low-temperature pyrolysis. According to earlier research (Shen and Gu 2009), the main composition of bio-oil from the thermal decomposition of cellulose includes 5-hydromethylfurfural, furfural, and hydroxylacetone. The cited authors concluded that the furfural was mainly produced by the secondary reaction of 5-hydromethylfurfural.

**Table 2.** Identification of Product Composition by Py-GC/MS

Retention time (min)	Products name	Formula	Yield, Area percent/ (%)				
			400°C	500°C	600°C	700°C	800°C
8.89	2-Cyclopenten-1-one	C <sub>5</sub> H <sub>6</sub> O	6.27	8.06	9.77	-	-
8.91	Benzene, 1-ethenyl-3-methyl-	C <sub>9</sub> H <sub>10</sub>	-	-	-	10.25	3.67
9.08	2-Cyclopenten-1-one, 2-methyl-	C <sub>6</sub> H <sub>8</sub> O	-	6.73	4.52	-	-
10.23	Benzene, 1-methoxy-4-methyl-	C <sub>8</sub> H <sub>10</sub> O	-	2.68	-	-	-
10.47	Acetic acid	C <sub>2</sub> H <sub>4</sub> O <sub>2</sub>	2.27	-	-	-	-
10.72	Furfural	C <sub>5</sub> H <sub>4</sub> O <sub>2</sub>	30.99	21.93	9.23	-	-
11.06	Indene	C <sub>9</sub> H <sub>8</sub>	-	-	7.92	17.91	15.23
11.48	Benzofuran	C <sub>8</sub> H <sub>6</sub> O	-	-	5.10	10.05	8.02
11.70	Pyrrole	C <sub>4</sub> H <sub>5</sub> N	6.19	6.89	4.24	8.50	8.30
11.83	Benzaldehyde	C <sub>7</sub> H <sub>6</sub> O	-	-	-	5.41	3.97
13.48	Benzonitrile	C <sub>7</sub> H <sub>5</sub> N	-	-	-	-	5.30
13.69	Benzaldehyde, 2-methyl-	C <sub>8</sub> H <sub>8</sub> O	-	3.34	-	-	-
14.53	2-Furanmethanol	C <sub>5</sub> H <sub>6</sub> O <sub>2</sub>	8.31	4.67	-	-	-
15.76	Naphthalene	C <sub>10</sub> H <sub>8</sub>	-	-	-	5.52	29.52
16.14	Oxime, methoxy-phenyl-	C <sub>8</sub> H <sub>9</sub> NO <sub>2</sub>	10.24	-	-	-	-
17.46	Guaiacol	C <sub>7</sub> H <sub>8</sub> O <sub>2</sub>	15.14	12.18	-	-	-
19.19	Phenol	C <sub>6</sub> H <sub>6</sub> O	20.32	21.33	37.34	36.20	17.01
20.00	Phenol, 4-methyl-	C <sub>7</sub> H <sub>8</sub> O	-	3.89	15.19	6.43	-
20.94	Phenol, 4-ethyl-	C <sub>8</sub> H <sub>10</sub> O	-	5.31	6.67	-	-
21.16	Acenaphthylene	C <sub>12</sub> H <sub>8</sub>	-	-	-	-	2.32
22.96	Benzofuran, 2,3-dihydro-	C <sub>8</sub> H <sub>8</sub> O	-	3.00	-	-	-

When the pyrolysis temperature increased from 500°C to 600°C, the yield of furfural decreased from 21.93% to 9.23%; as pyrolysis temperature increased from 600°C to 700°C, furfural compound products disappeared. With the increase of temperature, the volatiles will undergo secondary reactions (Jegers and Klein 1985; Fenner and Lephardt 1981). Therefore, the yield of furfural decreased with increasing temperature and was mainly caused by the second reactions.

Meanwhile, guaiacol and phenol were the typical products of lignin pyrolysis (Patwardhan *et al.* 2011). From Table 2, no guaiacol product was detected by GC/MS when the set pyrolysis temperature was higher than 600 °C. However, the yield of phenol was the highest from tobacco stem pyrolysis at 600°C. These results indicated that the methoxy group of guaiacol was decomposed at 600°C, and then guaiacol was transformed to phenol. When the pyrolysis temperature increased to 700°C and 800°C, the

main components of pyrolysis were phenol, indene, and naphthalene. The yields of indene and naphthalene increased with increasing pyrolysis temperature. The highest yields of indene and naphthalene occurred at 700°C and 800°C, where the maxima were 17.91% and 29.52%, respectively. It can be concluded that the pyrolysis temperature had a significant effect on the formation of furfural, indene, and naphthalene, but obviously had no effect on the yield of phenol.

An important compound, benzonitrile, was also characteristic of tobacco stem pyrolysis at 800°C. Benzonitrile is known to be highly toxic. Therefore, the most suitable pyrolysis temperature of tobacco stem should be lower than 800°C to avoid its formation. On the other hand, relatively high amounts of furfural, 2-methoxyphenol, and phenol were produced at low pyrolysis temperatures. Therefore, tobacco stem produced furfural and phenol compounds at low temperature pyrolysis conditions, which may be a novel utilization approach.

### TG and DTG Analysis

The curves of TG and the rate of thermal degradation (DTG) from tobacco stem pyrolysis are shown in Fig. 1. Based on the DTG profile, the pyrolysis process of tobacco stem could be divided into three stages. The first stage, below 150°C, was responsible for the drying process; the maximum mass loss rate for this stage occurred at 103°C.

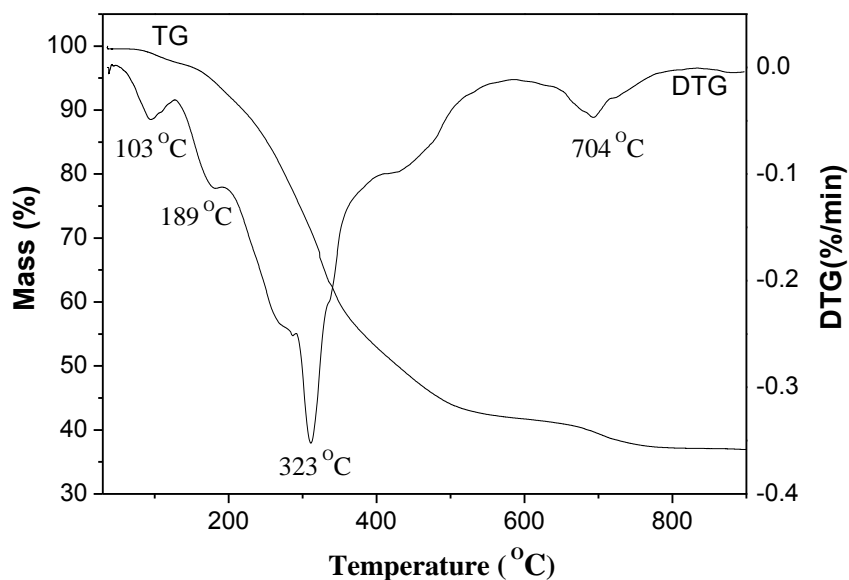


Fig. 1. TG and DTG curves of tobacco stem

The second stage was a fast thermal decomposition process for tobacco stem, accounting for 59.98 wt. % weight loss. There were two peaks in the DTG curve at this stage; the temperature for the first peak was 189°C, while the maximum weight loss rate occurred at the second peak at 323°C. According to Baliga *et al.* (2003), pectin showed initial melting as early as 150°C and a total melt by 250°C. Meanwhile, hemicellulose started to decompose at a temperature near 450 K (Navarro *et al.* 2009). This indicated that the peak at 189°C may be caused by the decomposition of pectin and hemicellulose.

According to Biagini *et al.* (2006) and Yang *et al.* (2007), cellulose exhibits the highest mass loss among the three main components of biomass, and the weight loss

attributable to cellulose was in the range 315 to 400°C. However, lignin was more difficult to decompose, as its weight loss occurred in a wider temperature range than other components. In this study, the cellulose, hemicellulose, and lignin content of tobacco stem were 39.01%, 5.05%, and 6.51%, respectively. So, the main weight losses at 300 to 400°C were mainly caused by the devolatilization of cellulose. Base on FTIR analysis (Figs. 2 and 3), the volatile release in the stage mainly were alkanes and CO<sub>2</sub>, which were released from the decomposition of cellulose (Statheropoulos and Kyriakou 2000; Banyasz *et al.* 2001).

The third mass loss stage was due to the charring of the residue, which encompassed a wider temperature range of around 500°C to 950°C and accounted for 8.42 wt. % weight loss. The maximum mass loss rate in the third stage was observed at 704°C. The total weight loss of all three stages was 68.40 wt. %. Earlier reports (Ahamad and Alshehri 2012; Xia *et al.* 2011) noted that the carbon yield of tobacco stem pyrolysis was about 30% after heating to 900°C. The low carbon yield from tobacco stem pyrolysis indicated that this process was inefficient at converting this biomass waste into activated carbon.

### FTIR Analysis of Evolved Volatiles

The evolved volatiles from the TG measurements were captured in a FTIR glass cell and monitored by FTIR in real-time. The IR absorbance information of products at various wave numbers and evolution times is shown in Fig. 2. According to earlier reports (Liu *et al.* 2008), the unique existence of characteristic bands in the wave number ranges of 2260 to 1990 and 2550 to 2450 cm<sup>-1</sup> were assigned to CO and CO<sub>2</sub>, respectively. The formation of CO and CO<sub>2</sub> followed two steps. At first, the generation of CO and CO<sub>2</sub> was released between 500 s and 1500 s and was due to the cracking of ether bonds (Liu *et al.* 2008; Guo *et al.* 2012). Secondly, when the temperature reached 600°C, the absorbance intensity of CO still existed; the evolutions of CO and CO<sub>2</sub> might be caused by the secondary cracking of volatiles.

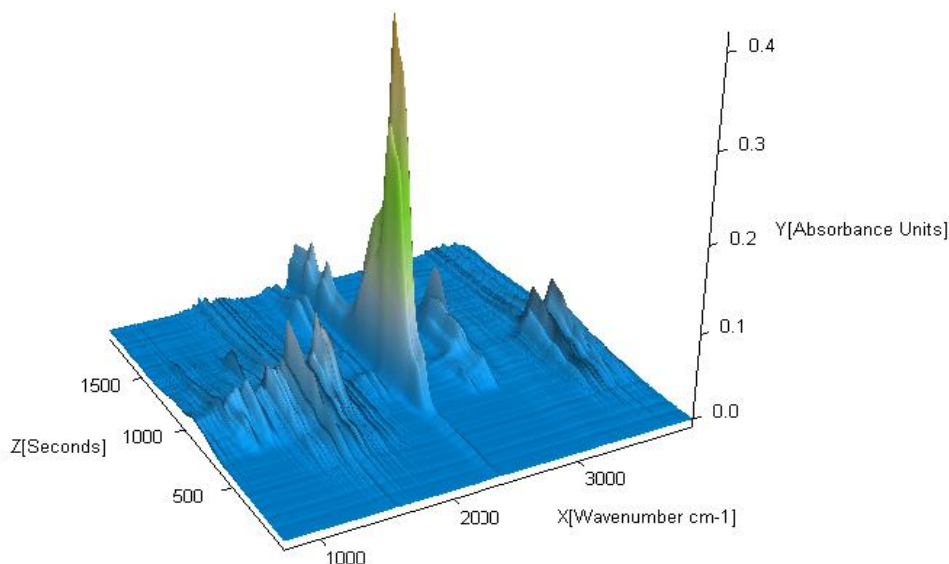
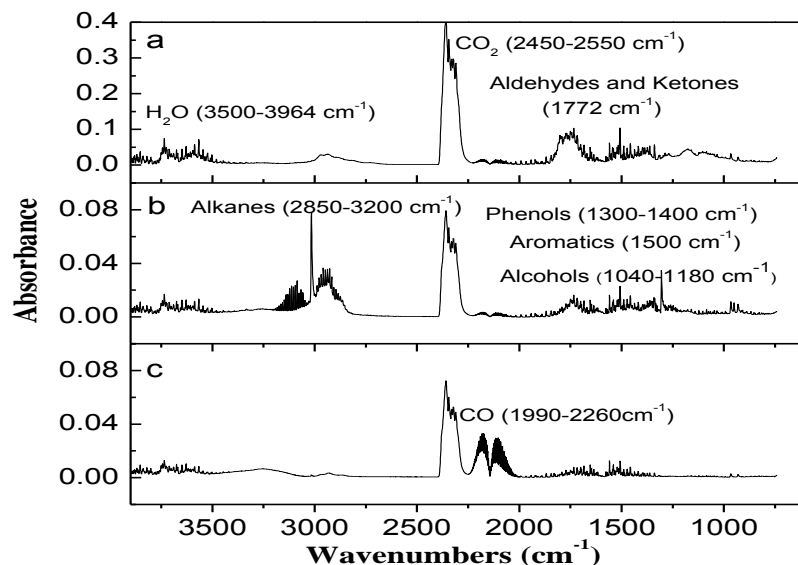


Fig. 2. FTIR spectra from tobacco stem pyrolysis over time

The characteristic bands between 1040 and 1180 cm<sup>-1</sup> indicated that alcohols were released (Lee and Fasina 2009). The intense signal cluster, centered on 1517 cm<sup>-1</sup> and

accompanied by signals at  $1772\text{ cm}^{-1}$ , strongly indicated the presence of aldehydes and ketones. The most significant band was the O-H absorption at  $1300$  to  $1400\text{ cm}^{-1}$ , corresponding to the presence of phenols. The bands at  $2850$ - $3200\text{ cm}^{-1}$  represented the existence of alkanes (Guo *et al.* 2011). According to Guo *et al.* (2012), alcohols were mainly released with cracking of the aromatic methoxyl groups and cinnamyl alcohol-type propanoid side chains; aldehydes and ketones were probably attributable to the  $C_{\beta}$ - $C_{\gamma}$  cleavage of alkyl side chains with  $-\text{CH}_2\text{OH}$  or  $-\text{COOH}$  groups in  $\gamma$  position. Meanwhile, phenols were primarily produced from the cleavage of the ether bonds between the lignin phenylpropane units, followed by cracking and reforming of the alkyl side chains of these units. Therefore, the volatiles products, including CO,  $\text{CO}_2$ , phenols, alkanes, aldehydes, and ketones ( $\text{C}=\text{O}$ ) were evolved between  $500\text{ s}$  ( $167^\circ\text{C}$ ) and  $1500\text{ s}$  ( $500^\circ\text{C}$ ). The release of these products mainly occurred at low temperatures, corresponding to the main pyrolysis temperature zone in the TG curve (Fig. 1).

In this work, the characteristic temperatures such as the initial and terminal temperatures of main pyrolysis stage, the temperature at the maximum weight loss rate of char pyrolysis stage were determined by DTG curves. Based on the DTG curves, three temperature levels were selected to investigate the components of volatile products and the formation mechanisms of main products. The spectra of volatiles released at  $300^\circ\text{C}$ ,  $407^\circ\text{C}$ , and  $704^\circ\text{C}$  are shown in Fig. 3a, b, and c, respectively.



**Fig. 3.** FTIR spectra of volatile products at the maximum weight loss rate. (a) FTIR spectrum of volatiles released at  $300^\circ\text{C}$ . (b) FTIR spectrum of volatiles released at  $407^\circ\text{C}$ . (c) FTIR spectrum of volatiles released at  $704^\circ\text{C}$

As shown in Fig. 3a, in the initial pyrolysis stage, the mass loss was primarily caused by the release of  $\text{CO}_2$ ,  $\text{H}_2\text{O}$ , aldehydes, and ketones. However, in the terminal pyrolysis stage, the weight loss was ascribed to the evolutions of alkanes,  $\text{CO}_2$ , alcohols, aromatics, and phenols (Fig. 3b). It can be found that the species of volatile products in the initial and terminal pyrolysis stage were different. It was reasonable to postulate that the volatilization of aldehydes and ketones occurred at lower temperatures than the volatilization of alcohols, alkanes, aromatics, and phenols.

As shown in Figs. 3a and b, the absorption band of CO<sub>2</sub> was more obvious than other volatilized products, and when the reaction progressed into the char pyrolysis stage, the absorption band of CO<sub>2</sub> still existed (Fig. 3c). This indicated that a considerable amount of CO<sub>2</sub> was continuously released during the entire pyrolysis stage. From Fig. 3c, the release of large molecular volatile products was not as prominent, while the formation of CO was dominant. Based on previous researches (Greenwood *et al.* 2002; Liu *et al.* 2008), the releasing of CO at higher temperature was primarily caused by the dissociation of diaryl ether and the secondary cracking of volatiles.

### MS Analysis of Evolution Patterns of Volatile Products

To determine the ion species from TG-MS, the major ionic fragments of Py-GC/MS analysis (Table 2) were used to select specific ion species (*m/z*) for real-time generation profiles of pyrolysis products. The real-time evolution curves of furfural, phenol, guaiacol, 4-methylformaldehyde, benzaldehyde, indene, and naphthalene from TG/MS analysis are shown in Fig. 4.

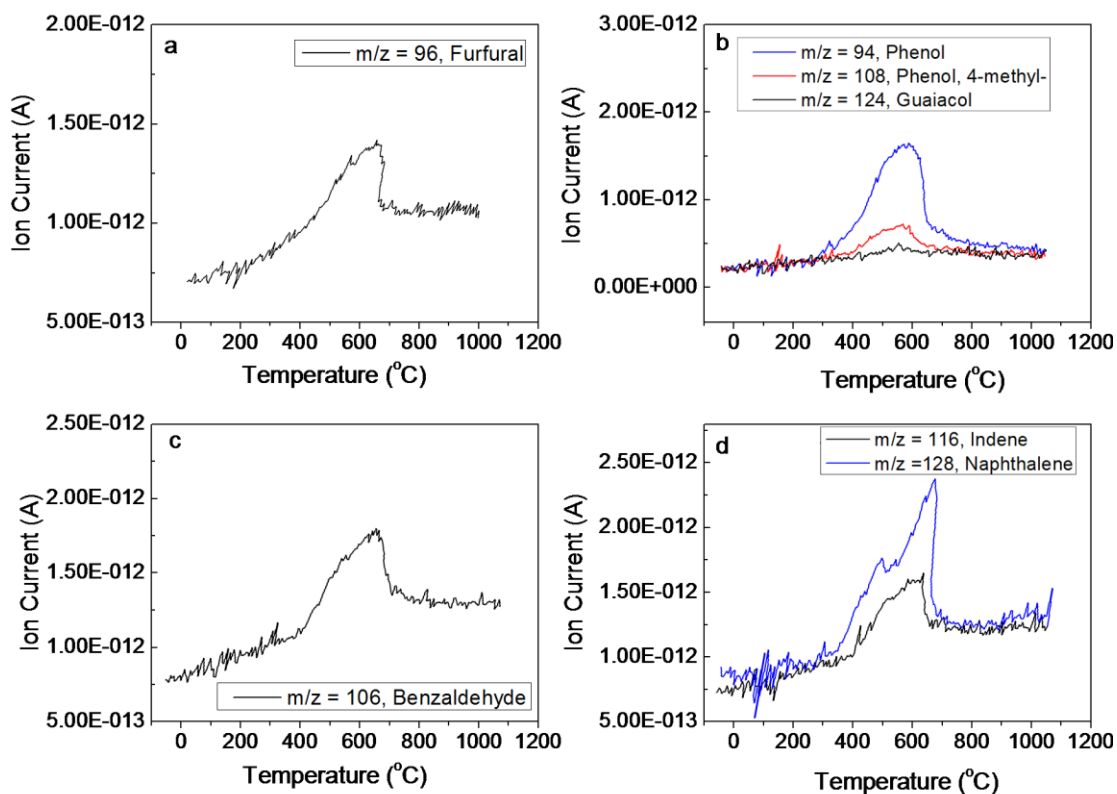


**Fig. 4.** Evolved gas analysis plots of the characteristic MS fragments from tobacco stem pyrolysis

From Fig. 4a, furfural, the major product of low temperature pyrolysis, started to evolve around 300°C, then reached a maximum around 500°C, and drastically decreased around 600°C. Similarly, phenol, another major product, began to evolve about 400°C and reached a maximum amount about 550°C. Meanwhile, as shown in Fig. 4b, the evolution curves of guaiacol and 4-methylphenol were similar to that of phenol. The difference between phenol and 4-methylphenol was the amount. From the comparison of the curves in Figs. 4a and b, it could be observed that furfural reached the maximum

evolution at lower pyrolysis temperature than phenol. According to the literature (Banyasz *et al.* 2001), the generation of furfural compounds is due to the pyrolysis of the cellulose component, while the evolution of phenols is attributed to lignin pyrolysis. Therefore, these observations indicated that the cellulose component of tobacco stem pyrolysis dominated at the lower reaction temperatures and the lignin component of tobacco stem pyrolysis dominated at higher reaction temperatures. The evolution profile of benzaldehyde as a function of peak temperatures is shown in Fig. 4c. Benzaldehyde started to evolve around 350°C, reaching a maximum around 550°C. The evolution curve of benzaldehyde appeared to be similar to that of furfural.

By comparing the formation temperature ranges of indene and naphthalene in stepwise Py-GC/MS and TG/MS analysis, the TG/MS operated at a fixed heating rate mode and provided more opportunity in the evolution pattern than the Py-GC/MS which operated in flash heating rate mode. The evolution pattern of indene resembled that of naphthalene and started to release about 400°C; however, the formations of indene and naphthalene were detected by Py-GC/MS till 700°C. It can be surmised from these results that fast pyrolysis of tobacco stem postponed the generation of indene and naphthalene.

## CONCLUSIONS

TG-FTIR, TG-MS, and Py-GC/MS techniques were used to study the pyrolysis mechanisms of tobacco stem. The compositions of pyrolysis products were determined by Py-GC/MS analysis. The evolution pattern of volatiles was revealed by the comparative study of TG-FTIR and TG-MS. The major composition of pyrolysis products by Py-GC/MS were furfural, phenol, indene, and naphthalene. The major volatiles from tobacco stem pyrolysis by TG-FTIR occurred between 167°C and 500°C, and were CO, CO<sub>2</sub>, phenols, aldehydes, and ketones. The indene and naphthalene formation temperature of fast pyrolysis is obviously higher than that of slow pyrolysis.

## ACKNOWLEDGMENTS

This work was supported by the China National Tobacco Corporation Program of Science and Technology (China Tobacco Office 2011-151), Guangdong Tobacco Corporation Program of Science and Technology (Guangdong Tobacco Office 2011-6), the National Natural Science Foundation of China (NSFC, No. 21176095), the National High Technology Research and Development Program of China (863 Program, 2012AA101806), and the Major Research Projects of Guangdong Province, China (No. 2011A090200006).

## REFERENCES CITED

- Ahamad, T., and Alshehri, S. M. (2012). "TG-FTIR-MS (evolved gas analysis) of bidi tobacco powder during combustion and pyrolysis," *Journal of Hazardous Materials* 199-200(15 January 2012), 200-208.
- Banyasz, J. L., Li, S., Lyons-Hart, J., and Shafer, K. H. (2001). "Gas evolution and the mechanism of cellulose pyrolysis," *Fuel* 80(12), 1757-1763.

- Baliga, V., Sharma, R., Miser, D., McGrath, T., and Hajaligol, M. (2003). "Physical characterization of pyrolyzed tobacco and tobacco components," *Journal of Analytical and Applied Pyrolysis* 66(1), 191-215.
- Biagini, E., Barontini, F., and Tognotti, L. (2006). "Devolatilization of biomass fuels and biomass components studied by TG/FTIR technique," *Industrial & Engineering Chemistry Research* 45(13), 4486-4493.
- Czernik, S., and Bridgwater, A. (2004). "Overview of applications of biomass fast pyrolysis oil," *Energy & Fuels* 18(2), 590-598.
- Fenner, R. A. and Lephardt, J. O. (1981). "Examination of the thermal decomposition of kraft pine lignin by Fourier transform infrared evolved gas analysis," *Journal of Agricultural and Food Chemistry* 29(4), 846-849.
- French, R., and Czernik, S. (2010). "Catalytic pyrolysis of biomass for biofuels production," *Fuel Processing Technology* 91(1), 25-32.
- Greenwood, P. F., Van Heemst, J. D. H., Guthrie, E. A., and Hatcher, P. G. (2002). "Laser micropyrolysis GC-MS of lignin," *Journal of Analytical and Applied Pyrolysis* 62(2), 365-373.
- Guo, D. L., Wu, S. B., Liu, B., Yin, X. L., and Yang, Q. (2012). "Catalytic effects of NaOH and Na<sub>2</sub>CO<sub>3</sub> additives on alkali lignin pyrolysis and gasification," *Applied Energy* 95(July 2012), 22-30.
- Guo, D. L., Wu, S. B., Lou, R., Yin, X. L., and Yang Q. (2011). "Effect of organic bound Na groups on pyrolysis and CO<sub>2</sub>-gasification of alkali lignin," *BioResources* 6(4), 4145-4157.
- Heo, H. S., Park, H. J., Park, Y. K., Ryu, C., Suh, D. J., Suh, Y. W., Yim, J. H., and Kim, S. S. (2010). "Bio-oil production from fast pyrolysis of waste furniture sawdust in a fluidized bed," *Bioresource Technology* 101(1), S91-S96.
- Jegers, H. E., and Klein, M. T. (1985). "Primary and secondary lignin pyrolysis reaction pathways," *Industrial & Engineering Chemistry Process Design and Development* 24(1), 173-183.
- Kayıkçıoğlu, H. H., and Okur, N. (2011). "Evolution of enzyme activities during composting of tobacco waste," *Waste Management & Research* 29(11), 1124-1133.
- Lee, S., and Fasina, O. (2009). "TG-FTIR analysis of switchgrass pyrolysis," *Journal of Analytical and Applied Pyrolysis* 86(1), 39-43.
- Li, W., Zhang, L., Peng, J., Li, N., and Zhu, X. (2008). "Preparation of high surface area activated carbons from tobacco stems with K<sub>2</sub>CO<sub>3</sub> activation using microwave radiation," *Industrial Crops and Products* 27(3), 341-347.
- Li, X., Lv, Y., Ma, B., Jian, S., and Tan, H. (2011). "Thermogravimetric investigation on co-combustion characteristics of tobacco residue and high-ash anthracite coal," *Bioresource Technology* 102(20), 9783-9787.
- Liu, Q., Wang, S., Zheng, Y., Luo, Z., and Cen, K. (2008). "Mechanism study of wood lignin pyrolysis by using TG-FTIR analysis," *Journal of Analytical and Applied Pyrolysis* 82(1), 170-177.
- Mohan, D., Pittman, C. U., and Steele, P. H. (2006). "Pyrolysis of wood/biomass for bio-oil: A critical review," *Energy & Fuels* 20(3), 848-889.
- Navarro, M. V., Murillo, R., Mastral, A. M., Puy, N., and Bartroli, J. (2009). "Application of the distributed activation energy model to biomass and biomass constituents devolatilization," *AIChE Journal* 55(10), 2700-2715.

- Pütün, A. E., Önal, E., Uzun, B. B., and Özbay, N. (2007). "Comparison between the "slow" and "fast" pyrolysis of tobacco residue," *Industrial Crops and Products* 26(3), 307-314.
- Piotrowska, A., Olejnik, A., Cyplik, P., Dach J., and Czarnecki, Z. (2009). "The kinetics of nicotine degradation, enzyme activities and genotoxic potential in the characterization of tobacco waste composting," *Bioresource Technology* 100(21), 5037-5044.
- Purwono, S., Murachman, B., Wintoko, J., Simanjuntak, B., Sejati, P., Permatasari, N. and Lidyawati, D. (2011). "The effect of solvent for extraction for removing nicotine on the development of charcoal briquette from waste of tobacco stem," *Journal of Sustainable Energy & Environment* 2(2011), 11-13.
- Patwardhan, P. R., Brown, R. C., and Shanks, B. H. (2011). "Understanding the fast pyrolysis of lignin," *ChemSusChem* 4(11), 1629-1636.
- Statheropoulos, M., and Kyriakou, S. A. (2000). "Quantitative thermogravimetric-mass spectrometric analysis for monitoring the effects of fire retardants on cellulose pyrolysis," *Analytica Chimica Acta* 409(2000), 203-214.
- Sung, Y. J., and Seo, Y. B. (2009). "Thermogravimetric study on stem biomass of *Nicotiana tabacum*," *Thermochimica Acta* 486(1-2), 1-4.
- Shen, D., and Gu, S. (2009). "The mechanism for thermal decomposition of cellulose and its main products," *Bioresource Technology* 100(24), 6496-6504.
- Xia, X., Liu, H., Shi, L., and He, Y. (2011). "Tobacco stem-based activated carbons for high performance supercapacitors," *Journal of Materials Engineering and Performance* 20(9), 1-6.
- Yang, H., Yan, R., Chen, H., Lee, D. H., and Zheng, C. (2007). "Characteristics of hemicellulose, cellulose and lignin pyrolysis," *Fuel* 86, 1781-1788.
- Yang, Z., Zhang, S., Liu, L., Li, X., Chen, H., Yang, H., and Wang, X. (2012). "Combustion behaviours of tobacco stem in a thermogravimetric analyser and a pilot-scale fluidized bed reactor," *Bioresource Technology* 110(April 2012), 595-602.

Article submitted: August 23, 2012; Peer review completed: October 27, 2012; Revised version received: November 14, 2012; Accepted: November 16, 2012; Published: November 21, 2012.